Interaction of Two Amphipathic α-Helix Bundle Proteins, ApoLp-III and ApoE 3, With the Oil-Aqueous Interface

Mona Mirheydari[1], Priya Putta[2], Elizabeth K. Mann[1], Edgar E. Kooijman[2*]

Kent State University, [1]Physics Department, and [2]Department of Biological Sciences, PO Box 5190, Kent, OH 44242

[*]corresponding author, ekooijma@kent.edu

Mona Mirheydari currently at:

University of Cincinnati
Department of Internal Medicine
Division of Cardiovascular Health and Disease
231 Albert Sabin Way, ML 0542
Cincinnati, OH, USA 45267-0542

Priya Putta currently at:

Cleveland Clinic Lerner Research Institute,
Department of Biomedical Engineering
9620 Carnegie Ave. ND building
Cleveland, OH, USA 44195-0001

Abstract

Protein-lipid interactions govern the structure and function of lipoprotein particles, which transport neutral lipids and other hydrophobic cargo through the blood stream. Apolipoproteins cover the surface of lipoprotein particles, including low density (LDL) and high density (HDL) lipoproteins, and determine their function. Previous work has focused on small peptides derived from these apolipoproteins or used such artificial lipid systems as Langmuir monolayers or the lipid disc assay to determine how apolipoproteins interact with the neutral lipid interface. Here we focus on a recurring protein domain found in many neutral lipid binding proteins, the amphipathic α-helix bundle. We use liquid-droplet tensiometry to investigate protein-lipid interactions on an oil droplet, which mimics the real lipoprotein interface. The N-terminus of apoE 3 and full length apoLp-III serve as model proteins. We find that each protein interacts with lipid monolayers at the oil-aqueous interface in unique ways. For the first time we show that helix bundle unfolding is critical for proper protein insertion into the lipid monolayer at the oil-aqueous interface, and that specific membrane lipids promote the rebinding of protein upon fluctuation in droplet size. These results shed new light on how amphipathic apolipoprotein α-helix bundles interact with neutral lipid particles.

Introduction

Apolipoproteins are amphipathic molecules that bind to lipids and form lipoproteins. Apolipoproteins act as lipid carriers, enzyme cofactors, ligands for cell membrane receptors, and structural components of lipoproteins. Mutation in the apolipoprotein structure result in abnormal lipid metabolism, which results in various diseases (*1*). Thus, understanding the mechanisms through which proteins bind to neutral lipid particles is important. Further, investigation of these

proteins sheds light on the role of the hydrophobic surface in lipid-protein interaction more generally.

Mammalian lipoproteins have a hydrophobic core rich in triacylglycerol and some cholesterol esters. A phospholipid monolayer surrounds the hydrophobic core, and apolipoproteins are attached to the lipoprotein surface. Lipoproteins transport nutrients that are insoluble in water through the blood stream to peripheral tissues. The apolipoproteins present on the surface of lipoprotein particles depend on the type of lipid particle. All apolipoproteins share amphipathic α-helices as a common structural feature (*2, 3*). In several of these apolipoproteins, the amphipathic α-helices organize into a helix bundle when the protein is not bound to lipid. Examples of such proteins are apoA1, apoE and apoLp-III. The α-helix bundle may facilitate protein binding to the phospholipid monolayer (*4, 5*). Prevost et al., show that large hydrophobic residues are critical for the amphipathic α-helices to bind to the phospholipid monolayer surrounding the structurally similar lipid droplet (*6*).

Here, we focus on the role of amphipathic α-helix bundles in the association of exchangeable proteins and lipid particles. To do so, we consider two different proteins associated with lipid particles and composed almost entirely of amphipathic α -helices. First, we consider the segment of mammalian apoE 3 that forms the α-helix bundle domain (henceforth named apoE 3 NT)). Second, we study apolipophorin-III (apoLp-III), an insect apolipoprotein. In order to further investigate the role of helix bundle unfolding we used a mutant of apoLp-III where two of the amino acid residues were replaced by cysteine residues (*7*) which inhibits the protein from unfolding. The two cysteine residues form a disulfide bond, which locks the hydrophobic residues located on the inner side of the helix (*7*).

Apolipoprotein E is a member of the mammalian apolipoprotein family that plays a role in the catabolism of the triacylglycerol-rich lipoprotein particles (*8-10*). The full-length protein has 299 amino acids. The N-terminus, amino acids 1-167, forms the amphipathic α-helix bundle domain with four anti-parallel amphipathic α-helices. This domain also includes the LDL receptor binding domain (residues 135 through 150) (*11*). The C-terminus, amino acids 191-299, also contains 3 large helices with hydrophobic surfaces. Residues 260 to 280 constitute the lipid targeting/binding domain (*11*).

ApoE was first recognized due to its importance in lipoprotein metabolism and cardiovascular disease. Deficiency in apoE causes hyperlipidemia type III, where the amount of plasma cholesterol and triacylglycerol increases due to accumulation of chylomicron, VLDL and LDL particles. Such individuals show a risk for premature atherosclerosis type 1 (*12*). ApoE has 3 isoforms which differ by a single amino acid residue (*11*). ApoE 3 is the most common type of apoE, present in over 75% of the population, whereas apoE 2 is the rarest (~8%). The presence of an allele of apoE 2 decreases the risk of Alzheimer`s disease and is a key determinant of longevity. On the other hand, the presence of apoE 4 increases the probability of developing early onset Alzheimer`s (*13, 14*).

ApoLp-III is an insect apolipoprotein that forms an anti-parallel amphipathic α-helix bundle with five helices arranged in an up-and-down topology. These helices are connected through hinges (*15*). The bundle motif stabilizes the protein in the hemolymph of the insect. Hydrophobic residues are mainly located in the inner surface of the protein while the hydrophilic residues are mainly exposed to the aqueous environment (*16*).

The apoLp-III protein can be found in the lipid-free or lipid-bound state in physiological conditions. In the lipid-free state, the intrinsic stability of the helix bundle is low, which facilitates interaction with lipid surfaces (*17, 18*). When complexes of apoLp-III and lipid form, the protein undergoes considerable changes in tertiary structure. The helix bundle unfolds exposing the hydrophobic residues to the lipid interface (*19, 20*).

Small et al. have pioneered the use of droplet tensiometry, which determines the oil-aqueous interfacial tension, to characterize the adsorption of protein to a triacylglycerol droplet (*21*). Using this technique, proteins such as apoB-100, which is present in larger lipoprotein particles such as VLDL and LDL (*22-24*), and apoC I and II have been extensively characterized (*25, 26*). Apolipoprotein A-I, an apolipoprotein that has an amphipathic α-helical domain, has also been studied extensively (*27-30*). Many human apolipoproteins are exchangeable proteins; they can move from one lipoprotein particle to another or to the surrounding aqueous environment (*31*).

Here we use liquid droplet tensiometry for the first time to study the insertion and dynamics of amphipathic helix bundle domains of apoLp-III and apoE 3 (apoE 3 NT) into phospholipid-coated triglyceride droplets. We use our homebuilt droplet tensiometer (*32*) to change the lipid packing on the surface of the oil droplet by varying the droplet volume and thus surface area. Additionally, we systematically change (increase and decrease) the oil droplet volume to study the stability of the protein adsorption at the interface. We find that both proteins have a strong affinity for the oil interface, and a phospholipid monolayer affects droplet binding in unique ways for each protein. These results shed light on the physiological role of these proteins and underscores the critical importance of helix bundle unfolding.

Material and Methods

Materials: *1. Protein:* ApoE 3 NT was a generous gift from Dr. Narayanaswami from the California State University Long Beach. We used the protocol provided to dissolve the protein. Protein was mixed with 2M DDT (to forbid disulfide bond formation from C112 a.a.) and 6M guanidine-HCl (gn-HCl), suspended in PBS buffer. The mixture was incubated for 1 hour at 37 °C, and then dialyzed to remove excess of gn-HCl for 48 hours (3 buffer changes). A Nanodrop 1-position spectrophotometer model ND-2000 was used to measure the concentration of the protein constructs.

ApoLp-III and mutated apoLp-III (locked helices) were a kind gift from Dr. Paul Weers from California State University Long Beach. The protein was provided in powder form. We used HPLC grade water (W5SK Fisher scientific) to suspend the protein. 1 mg of protein was dissolved in 1 mL of water, setting the final concentration for protein stock to 1 mg/mL.

2. Lipids: POG (1-palmitoyl-2-oleoyl-*sn*-glycerol), POPC (1-palmitoyl-2-oleoyl-*sn*-glycero-3-phosphocholine), POPE (1-palmitoyl-2-oleoyl-*sn*-glycero-3-phosphoethanolamine), POPA (1-palmitoyl-2-oleoyl-*sn*-glycero-3-phosphate (sodium salt)) were purchased from Avanti Polar Lipids (Alabaster, Alabama). Triolein glyceride was purchased from NU-Check Prep (MN). Thin layer chromatography was used regularly to test the purity of lipids. For this test, we use a solvent consisting of $CHCl_3$/ CH_3OH/H_2O (64 ml /25 ml /4 ml) for polar lipids and for neutral lipid we used C_6H_{12}/ $(C_2H_5)_2O$ (10:1). The physicochemical characteristics of the lipids are given in Table 1.

Lipid Abbreviation	Charge	Chains	T_m/T_H [°C]	"Curvature"
POG	Neutral	Mixed	NA	Negative, Induces H_{II} phase 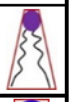
POPC	Zwitterionic	Mixed	-2	Infinite, forms Bilayer $C_0 = -0.022 \pm 0.010$ 1/nm 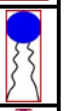
POPE	Zwitterionic	Mixed	25/71	Negative, forms H_{II} phase $C_0 = -0.316 \pm 0.007$ 1/nm 
POPA	Anionic	Mixed	28	Negative, Induces H_{II} phase 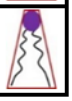

Table 1. The list of lipids used with relevant physicochemical properties. T_m is the melting temperature of the lipid bilayer from gel to fluid (Lα) phase, T_H is the transition temperature from the Lα phase to the hexagonal H_{II} phase. Spontaneous curvatures for POPC and POPE were taken from Kollmitzer et al. (35). Spontaneous curvature (C_0) for POG and POPA have not been determined, but can be estimated from that of related lipids: For DOG in water, C_0=-0.9 1/nm (33). For DOPA in water, C_0=-0.077 1/nm and in buffer at pH 7.4, C_0= -0.22 1/nm (34).

3. Chemicals: KCl, EDTA and Tris were purchased from Sigma Aldrich Co. All the chemicals were > 99% pure. HPLC-grade water was purchased from Fisher Scientific (WSK5). Salts were heated in an oven at 200 ^{0}C for 24 hours, to eliminate any organics.

Methods: *1. Buffer:* Tris buffer is made using 150 mM KCl, 10 mM Tris and 0.2 mM EDTA, carefully mixed in HPLC-grade water.

After buffer preparation, the buffer is kept in the experiment room (21.4 ± 0.2 °C) to assure the absence of temperature fluctuations and thus density variations. All glassware are cleaned using KOH cleaning solution (164 g ethanol, 25 g water and 24 g KOH).

2. Vesicle formation: Lipid films are made by drying 460 nmol of lipid in organic solution (chloroform or chloroform/methanol) under a stream of Nitrogen. The film is kept under vacuum for 24 hours to remove residual traces of organic solvent and was stored at -20 °C before use. Prior to vesicle formation, the lipid film is moved to room temperature for about 20 minutes. In order to form small unilamellar vesicles (SUV), 4 ml of water is used to suspend the lipid film. The mixture

is sonicated for 2 minutes using 12 cycles, where each cycle is 10 secs using a probe sonicator. The sample is kept on ice through the sonication process, to avoid heating the lipid mixture. Later the sample is centrifuged for 20 minutes to pellet the nano particles produced from the end of titanium probe (Qsonica Q55 sonicator). DLS (differential light scattering; Horiba 7100) is used to measure vesicles size. Normally the vesicles prepared this way are around 50 nm in size.

3. Liquid Droplet Tensiometer: Our homebuilt tensiometer is a combination of CCD camera (PixeLINK PL-B776F), light source (Thorlab), diffuser (Thorlab), syringe (Hamilton) with a J-shaped needle, and cuvette (made from borosilicate glass, supplied by Wale Apparatus PA, at a machine shop located in the Department of Chemistry, Kent State University) (*32*). A schematic is shown in supporting information Figure S1. The set-up is cleaned regularly using pure methanol to remove any organic residues. Syringe and needle are rinsed 3 times with chloroform for cleaning. The cuvette is cleaned using KOH solvent (164gr MeOH, 24 gr Water and 25 gr KOH), and rinsed with DI-water, and ultra-pure water a minimum of three times each. Two pumps are involved, one to vacuum water/buffer from the cuvette and the other one to fill the cuvette with fresh buffer/water. The syringe is attached to a micrometer screw (designed and fabricated by Wade Aldhizer in the machine shop in the Department of Physics at Kent State University) to manually control the volume of the droplet.

The surface tension, volume, droplet area and radius at apex are measured using the ADSA code package developed by the Neumann group at the University of Toronto (*36*). For a typical experiment, 3000 images are captured and analyzed simultaneously.

ADSA can be applied only to well-deformed droplets, which is quantified by calculating dimensionless Neumann numbers (Ne) (*37*):

$$Ne = \frac{\Delta\rho g R_0 H}{\gamma}$$

In this equation, R_0 is the radius of curvature at the drop apex and H is the drop height. Generally, larger drops, with a larger Ne,will have more deformed (elongated) shape, while smaller drops, with smaller Ne, will be more spherical. Stationary, uncoated droplets of triolein have relatively large interfacial tensions, and approximately 20 μL droplet volumes are ideal to ensure sufficiently well-deformed but stable droplets. The addition of a lipid monolayer and/or protein decreases the interfacial tension so that even smaller droplets become sufficiently elongated for reliable ADSA measurements. For example, a 5 μL drop of neat triolein in buffer yields Ne~0.5, which is insufficient for reliable interfacial tension measurements by ADSA. For a drop of the same size but coated with POPC, we estimate $Ne \sim 0.7$, which is sufficiently large that the interfacial tension determined by ADSA becomes nearly independent of droplet size (*38*). In the experiments discussed here, all small droplets were both ≥6 μL and sufficiently deformed ($Ne \sim 0.7 - 1$). Additional details on image analysis are given in (*32*).

Results

We present two general types of experiments. The first set of experiments, performed at steady state, investigates the influence of different lipids on the affinity and the cooperativity of protein binding to the triolein/aqueous interface. These are called protein insertion experiments. These experiments are performed with both proteins and the mutant. In a separate set of experiments, one protein is chosen for dynamic measurements, in which the surface area is oscillated to test the stability of the protein at the interface, as well as the influence of the protein on lipid stability.

Typical protein insertion experiment.

In all these experiments, a triolein droplet is first coated with phospholipid monolayer, to represent the lipoprotein surface. Lipids are chosen partially based on studies of the lipid

composition of the monolayer surrounding the lipid droplet (*39*). They are further chosen to have identical acyl chains while varying headgroup size and charge. These differences lead to a range of lipids with relevant physicochemical properties (see Table 1) (*32*). The PO (sn-1-palmitoyl, and sn-2-oleoyl) acyl chains were chosen because they are common in mammalian glycerophospholipid fatty acid compositions (*40*). Differences in the lipid headgroup also help clarify the effect of lipid-shape, i.e. spontaneous curvature, in lipid-protein interaction. All experiments are performed in buffer, i.e. 150 mM KCl, 10 mM Tris, and 0.1 mM EDTA set to pH 7.2 ± 0.5.

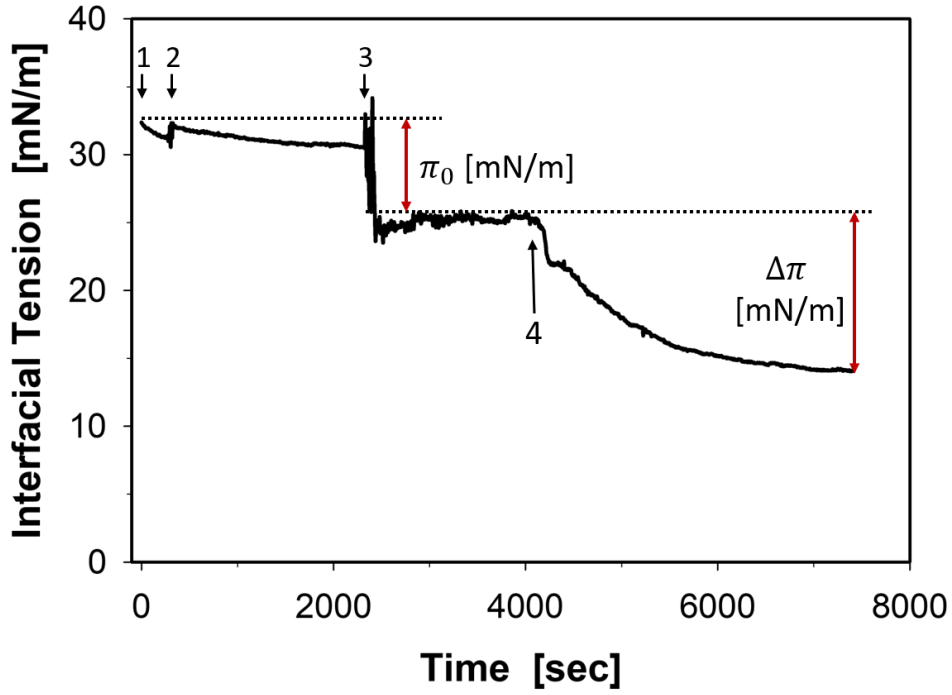

Figure 1. *A typical insertion experiment. 1) A droplet of triolein is formed. 2) After 5 min, 4 ml of the buffer in the cuvette is replaced by 4 ml of freshly made vesicles (here PC:PA.) Vesicles and oil droplet are left to interact for 30 min. 3) The droplet volume is changed to the desired value. Between 3 and 4, after stabilization of the lipid monolayer, the rest of the vesicles are rinsed out from the cuvette. 4) 0.1 nmol/L of the protein (here apoLp-III) is added to the cuvette. The droplet is incubated with the protein for 1 hr to let the protein interact with the oil interface.*

The monolayer insertion experiments follow the procedure by Donald Small (*22*). A typical experiment is shown in Figure 1. The cuvette is filled with 10 ml of buffer and a triolein droplet is formed at the end of a J-shaped needle. At this step (1) we then wait for at least 5 min until any drift in the surface tension is less than 0.2 mN/m per minute prior to further experimentation (between time point 1 and 2). At point 2, liposomes of either POPC or POPC mixed with 10 mol% of POPE, POG, or POPA are added. This is done by the removal of 4 ml of water/buffer from the top of the cuvette after which 4 ml of liposome solution is added cautiously. Deposition of the self-assembled phospholipid monolayer at the aqueous-oil interface is then followed via interfacial tension from time point 2 until 3 (where the spontaneous formation of a lipid monolayer has reached a steady state.) At this point 3, we compress the droplet surface by reducing the volume, followed, in the time period between points 3 and 4, by careful flushing with fresh buffer (50 mL in 10 min) to remove remaining lipid vesicles. A vacuum pump removes excess buffer from the top of the cuvette to keep the solution volume constant. At point 4, protein is added to a final concentration of 0.1 nmol/mL and left to interact with the oil/lipid interface until the interfacial tension again reaches steady state.

Two variables, π_0 and $\Delta\pi$ (see Fig. 1) are used to characterize the insertion data. π_0 is the decrease in interfacial tension due to the packing of the lipid alone; the droplet volume is decreased to reach the desired π_0 value. $\Delta\pi$ is the additional decrease in surface tension after protein addition. The effectiveness of protein insertion is deduced from the variation of $\Delta\pi$ as a function of the initial lipid pressure π_0.

The surface activity of apoLp-III was presented in an earlier article (*32*); 0.1 nmol/mL was more than sufficient to saturate the surface. For consistency with previous data for apoLp-III, we used 0.1 nmol/mL for both apoLp-III and apoE (NT) insertion studies.

Insertion of apoE 3(NT) and apoLp-III into different phospholipid monolayers at the oil/buffer interface.

The extent to which the protein adsorbs onto the lipid droplet to change its surface tension (by $\Delta\pi$) depends on the protein, on the lipids on the droplet surface, and on the packing of those lipids, characterized by the initial pressure π_0. Examples are given in Figure 2, with more examples in Figure S2 of the supporting information. Because $\Delta\pi$ is (within scatter) linear in π_0, these curves are usually characterized by two numbers (*32, 41*). The maximum insertion pressure (MIP), the x-intercept, indicates the monolayer pressure above which the protein no longer inserts (*42*). $\Delta\pi_{max}$, which is the extrapolation of $\Delta\pi$ to the limit where π_0 becomes zero, gives the maximal change in surface pressure when protein interacts with lipids at the monolayer interface. Any deviation of this value from $\Delta\pi$ due to the protein alone (red points in Figure 2) indicates how much the lipid facilitates or impedes the protein to come to the interface. The two parameters indicate the affinity of the protein for the lipid monolayer.

The values for the $\Delta\pi_{max}$, given in Table 2, demonstrate that both apoE and apoLp-III

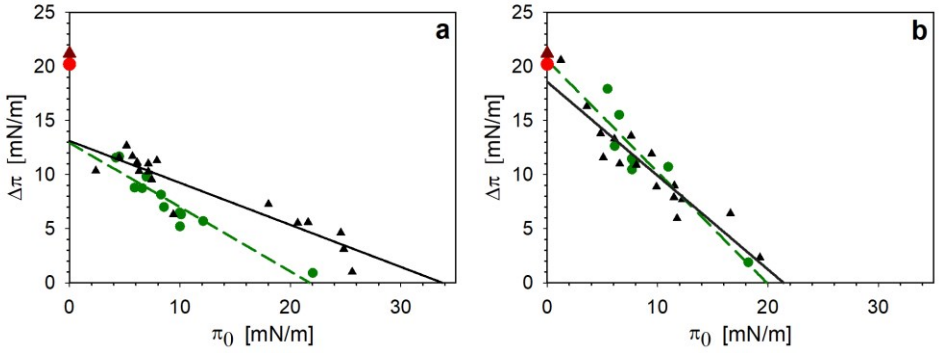

Figure 2. *Comparison of the insertion of apoE 3(NT) (green circles) and apoLp-III (black triangles) into a) POPC monolayers and b) POPC:POPA monolayers. Red circles/triangles correspond to the protein surface pressure without lipid monolayer. Tris buffer: 10mM Tris-HCl, 150 mM KCl, 0.2 mM EDTA at pH7.2.*

show the highest affinity toward the PC:PA monolayer. The affinity of the protein is significantly

lower with other lipid mixtures. In fact, for both proteins the other lipid mixtures show $\Delta\pi_{max}$ close to each other at ~12 and 14 mN/m for apoE 3 and apoLp-III respectively. These values are significantly less than the change in the surface pressure when the apoE 3 and apoLp-III interact with the bare triolein droplet.

The protein apoE 3 (NT) has the highest maximum insertion pressure (MIP) for the monolayer formed by PC:POG, with PC:PE close behind, while it shows the lowest MIP for PC:PA and POPC lipid mixtures. The protein apoLp-III shows the highest MIP for POPC and for PC:POG, with significantly lower values for PC:PA and PC:PE mixtures.

	apoE 3 (NT)		**apoLp-III**	
	MIP	**$\Delta\pi_{max}$**	**MIP**	**$\Delta\pi_{max}$**
POPC	**21.7±2.9**	**12.9±1.3**	**33.8±4.6**	**13.1±1.1**
PC:PA (9:1)	**19.9±4.1**	**20.6±3.5**	**21.4±2.7**	**18.6±1.8**
PC:PE (9:1)	**27.4±5.7**	**11.3±2.7**	**24.6±3.7**	**14.0±1.6**
PC:POG (9:1)	**31.6±4.7**	**12.1±1.2**	**30.3±4.2**	**15.6±1.5**

Table 2. Maximum insertion pressure (MIP) and $\Delta\pi_{max}$ calculated for the protein apoE 3 NT and apoLp-III in a physiologically relevant buffer, pH ~7.2.

Comparison of the insertion of locked (mutant) apoLp-III with native apoLp-III

Studies have demonstrated that apoLp-III unfolds its amphipathic α-helix bundle upon interactions with phospholipid (*7*). In order to investigate the importance of helix bundle unfolding

at the physiologically more relevant oil-phospholipid interface, we studied the insertion of a bundle-locked protein. In this mutant the helix bundle is modified by two cysteine residues in order to form a disulfide bond (*7*). The mutation of the protein was done on amino acids threonine (T) 36 and alanine (A) 136, as seen in Figure 3 a. The disulfide bond prevents the helix bundle from unfolding (*7*). The insertion experiments for this protein were performed as described above for the unlocked proteins.

$\Delta\pi$ (variation in surface pressure after protein insertion) decreased significantly with the locked protein at all π_0 (Figure 3 c.) The maximum insertion pressure, above which the protein

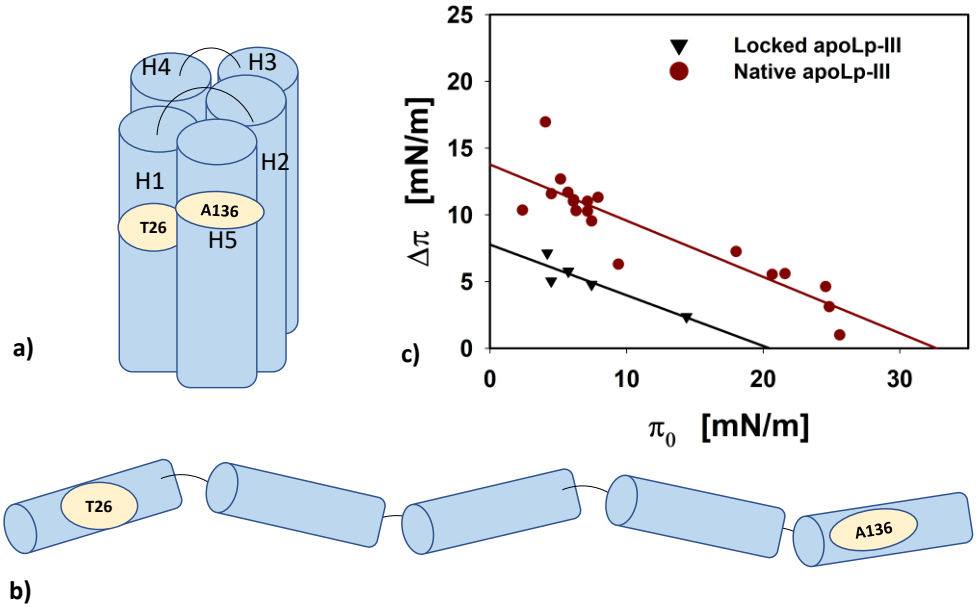

Figure 3. *a) Representation of the locked apoLp-III through mutation of T26 and A136. b) The schematic structure of the native protein. c) Comparison of the insertion of native apoLp-III (red circles) and locked apoLp-III (black triangles) into monolayers of POPC. Tris buffer: 10mM Tris-HCl, 150 mM KCl, 0.2 mM EDTA at pH7.2.*

cannot insert into the monolayer, $\Delta\pi_{max}$, reflecting the protein affinity, both decreased by ~10 mN/m for the mutant (locked) as compared to the native apoLp-III (unlocked) protein

Our data suggest that helix bundle unfolding plays a major role in protein interactions at the oil-phospholipid interface. Most of the hydrophobic residues are located in the interior of the helix bundle. Helix bundle unfolding allows the hydrophobic amino acid residues access to the hydrophobic surface of the oil droplet.

The dynamics of a protein-phospholipid film on a triolein droplet.

In the following studies, a lipid mixture is adsorbed to the surface, and a test protein, apoLp-III, inserted into the surface, as before. Here we perform compression/decompression cycles to study the stability of the adsorption. A major parameter of interest will be the hysteresis observed during those cycles. Depending on the lipid mixture, protein (absent or inserted), and environment (pure water vs. buffer), we observe both reversible hysteresis, in which compression and decompression of the surface follow different paths but successive cycles retrace the same paths, and irreversible hysteresis, in which successive cycles trace very different paths.

A typical experiment is shown in Figure 4. The cuvette is filled with 10 ml of water/buffer and a ~10 μl triolein droplet is formed at the end of the J-shaped needle (point 1 in the figure). The droplet is allowed to stabilize in the aqueous solution for at least 5 min prior to further experimentation. At point 2, liposomes of either pure POPC or POPC mixed with 10 mol% of POPE, POG, or POPA are added. This is done by the removal of 4 ml of water/buffer from the top of the cuvette after which 4 ml of liposome solution was added cautiously. Deposition of the self-assembled phospholipid monolayer at the aqueous-oil interface is then followed from time point 2 until 3. At this point (3), remaining vesicles are washed out by carefully flushing fresh water/buffer (50 mL in 10 min) through the cuvette. Water/buffer enters the bottom of cuvette through a needle

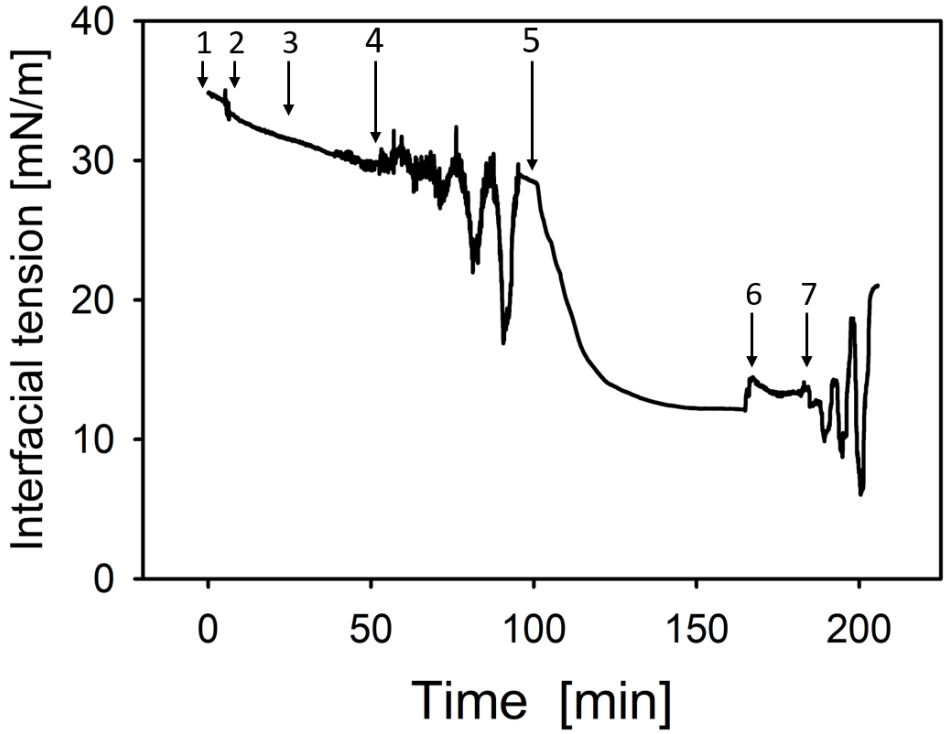

Figure 4. *Interfacial tension vs. time for a typical experiment: A triolein droplet was formed at the end of a J-shaped needle in water at point 1. At step 2, lipid liposomes (here POPC) are added. At step 3, remaining vesicles are flushed out. At step 4, we begin oscillating the droplet volume to give successive compression/decompression cycles. The protein (here apoLp-III) is added in step 5. In step 6, any remaining protein is flushed from the cell. In step 7, the droplet volume is again oscillated.*

connected to a peristaltic pump. To keep the volume of the solution in the cuvette constant, a vacuum pump removes excess water/buffer from the top of the cuvette.

Note that the interfacial tension does not change significantly during the removal of any remaining liposomes (between 3 and 4). At point 4, we start the successive compression and decompression cycles of the lipid droplet surface, by changing the droplet volume manually with the syringe (see methods).

During compression, the volume of the oil droplet, and thus its surface area, decreases, the lipid monolayer on the oil surface becomes more compact, and surface tension decreases (surface pressure increases.) During decompression, the oil droplet expands and with a larger surface area

available for the lipid molecules to relax, the tension increases (pressure decreases.) In order to characterize the stability of the lipid monolayer, several compression/decompression cycles are performed between specific droplet volumes. At the end of these cycles, the droplet volume is brought to its initial value, and the droplet is left at rest to stabilize.

At point 5, protein is added to reach a concentration of 0.1 nmol/mL in the cuvette and left to interact with the oil/lipid interface until the interfacial tension again reaches steady state. After 1 hr, any protein that does not bind to the oil interface is removed from the cuvette, step 6: 100 ml of buffer/water is flushed through the cell for approximately 20 min (between 6 and 7). While rinsing, any protein bound loosely to the lipid monolayer also detaches from the surface. This protein detachment is indicated on the graph by the variation in tension after rinsing. In step 7, we study the stability of the protein interaction with the oil-phospholipid monolayer interface by again oscillating the surface area. This process was run for lipid monolayers consisting of POPC, and POPC mixtures with 10mole% of POG, POPE and POPA in both water and buffer (i.e. 150 mM KCl, 10 mM Tris, and 0.1 mM EDTA set to pH 7.2 ± 0.5) subphases. Both water and buffer are investigated here to probe any electrostatic effects in protein interaction with the oil-phospholipid interface.

Dynamics of a triolein droplet coated with POPC interacting with apoLp-III.

The cylindrical, zwitterionic lipid, POPC, has both a positive and a negative charge. Figure 5a and 5c show compression/decompression isotherms for the oil droplet coated with a POPC lipid monolayer in water and buffer respectively. Figure 5b and 5d repeats Figure 5a and 5c respectively with the addition of apoLp-III protein to the interface.

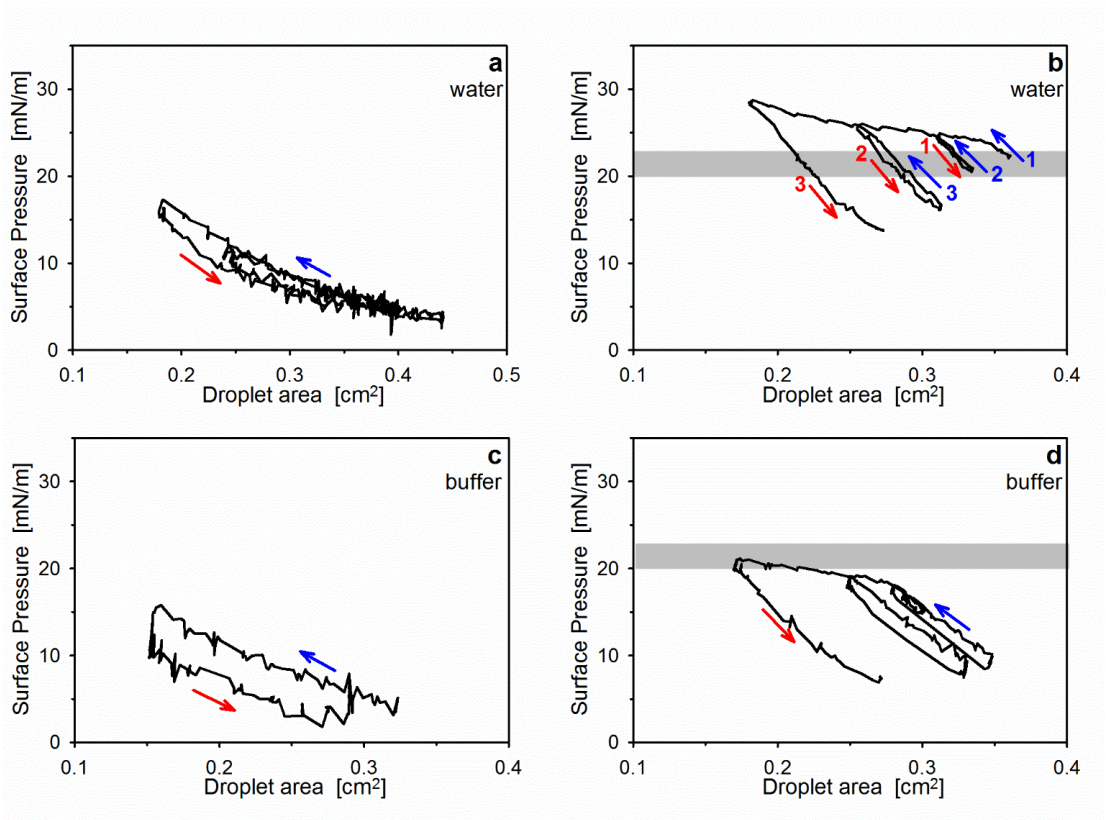

Figure 5. *Comparison of successive compression (blue arrow(s)) and decompression (red arrow(s)) isotherms for an oil droplet first after coating with POPC lipid (a,c), and then after apoLp III protein insertion (b,d). The same experiments are performed with the droplet in pure water (a,b) and in a physiologically relevant buffer, pH ~7.2 (c,d).*

For the lipid alone on the droplet surface in pure water, each successive cycle follows the same path, indicating that the compression/decompression of the lipid monolayer is reversible (Figure 5a.) The PC coated oil droplet in buffer could not undergo more than one oscillation cycle, Figure 5c, perhaps due to a higher level of hysteresis; further attempted changes in the droplet volume led to droplet detachment. In both media the decompression pathway is systematically below the compression one; the difference is bigger when the droplet sits in buffer (Figure 5c) than in pure water (Figure 5a). This area between the compression and decompression paths can be interpreted as the work required for the lipid molecules to reorganize during the

compression/decompression cycle (*24, 43, 44*). Thus, the larger areas correspond to major reorganization of the surface layers.

For the protein/POPC-coated oil droplet in water, the decompression/compression paths lie near each other, but at a significant distance from the next decompression path (Figure 5b, d.). In buffer, the decompression/compression paths lie further from each other, but closer to the next decompression path, until the surface area was reduced by a factor >1.5.

The maximum pressure attained with the lipid alone was similar in both water and buffer, ~15 mN/m. With the protein, the maximum pressure in pure water was much higher, ~27 mN/m, compared to ~20 mN/m in buffer (values are consistent with the work previously published (*32*)). Note that in buffer the maximum pressure is within uncertainties of the pressure for the protein on the pure oil-buffer interface, without phospholipid (indicated by the gray bars in Figure 5b and d). After several compression/decompression cycles, the minimum pressure reduced from 22 mN/m to 15 mN/m in pure water, while remaining at ~7 mN/m in buffer.

The dynamics on two of the phospholipid mixtures, PC:PE and PC:POG were qualitatively similar (Figure S3 and S4 in the Supporting Information.)

Dynamics of a triolein droplet coated with PC:PA (9:1) interacting with apoLp-III.

The set of compression/decompression experiments were then repeated with PC:PA mixtures (Figure 6); remember that PA has both negative charge and negative spontaneous curvature in contrast to PC (*34, 45, 46*). We observe significant differences in behavior compared to the pure POPC monolayer data (Figure 5) and the other lipid mixtures (given in the Supporting Information, in Figures S3-S4.)

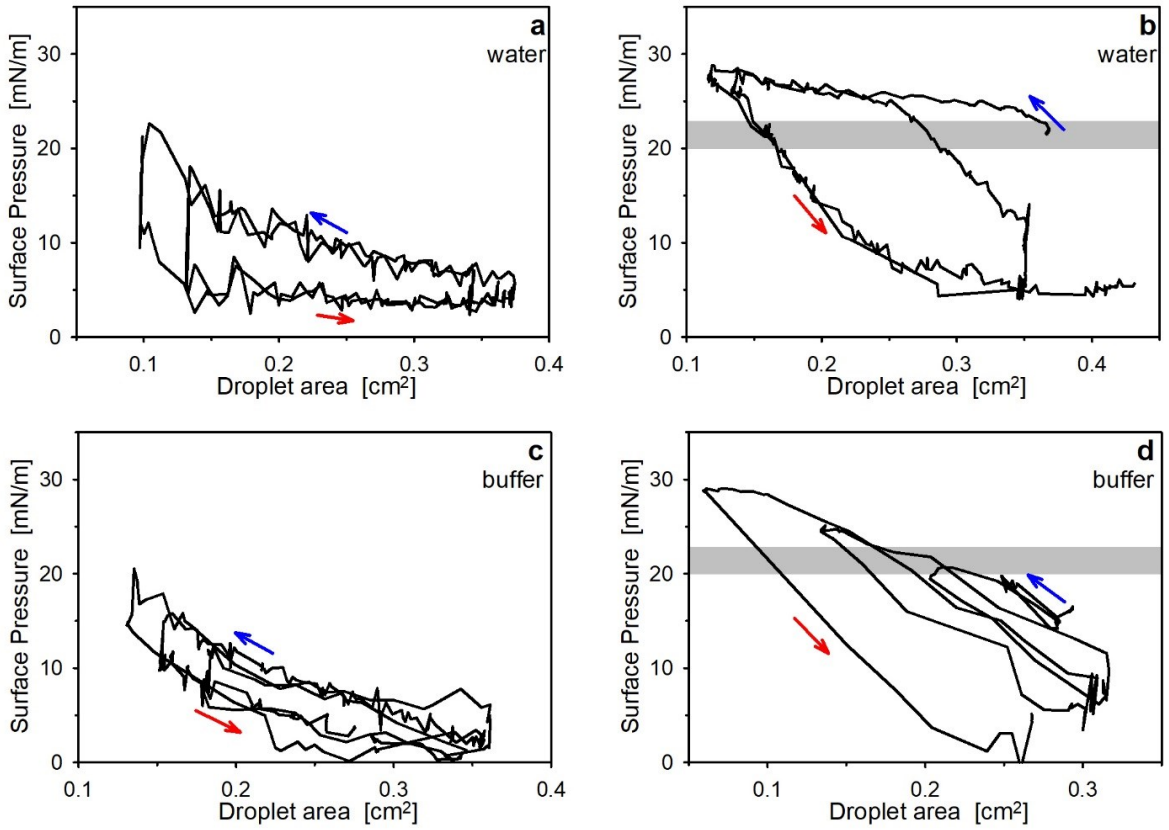

Figure 6. *Comparison of successive compression and decompression isotherms for an oil droplet first after coating with PC:PA (9:1) lipid mixture (a,c), and then after apoLp III protein insertion (b,d). The same experiments are performed with the droplet in pure water (a,b) and in a physiologically relevant buffer, pH ~7.2 (c,d).*

For the lipid alone on the droplet surface in both pure water and in buffer, each successive cycle follows the same path, indicating that the compression/decompression of the lipid monolayer is reversible (Figure 6 (a,b).) However, these cycles showed significant hysteresis in both cases, although much less in the buffer solution.

The maximum surface tension attained for the pure lipid monolayer was similar in pure water and in buffer: ~21 mN/m. With the addition of protein, the pressure saturates at higher values near 28 mN/m. Notice that this is significantly higher than the saturation pressure for the protein without phospholipid (gray bar in Fig 6b and d).

In water the decompression/compression cycles for apoLp-III interacting with the PC/PA monolayer is significantly different from the PC monolayer (Figure 5b). After the first compression subsequent cycles follow the same path but with large hysteresis between decompression and compression isotherms. The behavior in buffer on the other hand is similar as that observed on the pure POPC monolayer.

Discussion

The combination of static and dynamic results gives information about three important ways that the lipid mixture can influence the interaction of proteins at a lipoprotein interface. First, the lipids may help attract the protein to the interface. Second, the lipids may help or hinder the protein from inserting into the interface. Third, the lipids may influence the stability of the proteins at the interface as the droplets change size by taking up or shedding neutral lipid. For example, a phosphatidylcholine (PC) monolayer clearly facilitates the adsorption (insertion) of peptides derived from apoC I and II to the lipid particle surface (*25, 26*).

Here we investigated not just PC but also mixed lipid monolayers since different lipid characteristics may be important in these three different roles. POG and to a lesser extent POPE and POPA belong to a class of lipids with negative spontaneous curvature: they can be visualized as cone shaped, with a smaller head than tail area (see Table 1). This class of lipid is known (*47-50*) to facilitate the interaction of peripheral membrane proteins since defects around the lipid helps the insertion of the hydrophobic protein domain into the hydrophobic interior of the membrane bilayer. Similarly, the addition of these lipids to predominantly PC monolayers is likely to lead to "gaps" between the lipid headgroups to facilitate the insertion of the hydrophobic domain to the

lipid monolayer. The role these lipids play in apolipoprotein interaction with a neutral lipid particle has not been extensively investigated to date (*32*).

Attracting protein to the interface

The surface charge (electrostatic potential) may attract the protein to the interface. The oil droplet core consists of a neutral lipid, triolein. However, its surface is charged, probably negatively (*51, 52*). Lipids at the surface may change the sign and density of that charge. For example, PA is negatively charged, while PC and PE are net neutral, and POG is uncharged.

The measured $\Delta\pi_{max}$, which characterizes the effective affinity of the protein for the interface at the limit of low lipid concentration, is significantly greater for PC/PA monolayers than for monolayers in which all of the lipids are either neutral or net neutral, for both proteins. This indicates that negative charge attracts the proteins to the interface. Indeed, apoE 3(NT) has a strong net positive charge in the 4th amphipathic helix (see Supporting Information, Figure S5). However, depending on pH, apoLp-III tends to be net neutral, with a positive charge in helix 3 and a negative charge in helix 5 (see Supporting Information, Figure S6). On the other hand, some anionic residues (aspartic and glutamic acids) can be protonated at interfaces, thereby losing their negative charge. Hence, the net charge of a protein or peptide at a lipid interface depends strongly on the pKa of the interfacial amino acid residues in question. The actual charge of the protein at the interface is thus unknown. However, apoLp-III is clearly attracted to the net negatively charged interface, underscoring the importance of electrostatics for apoLp-III and apoE 3 NT recruitment.

Once the protein reaches the interface, the proteins must unfold. Indeed, we note that the mutant form of apoLp-III, whose 1st and 5th helices are locked, has a significantly lower $\Delta\pi_{max}$, even though the surface charge of the bundle is similar to the native protein. This clearly

establishes the critical importance of helix bundle unfolding for efficient lipid interaction (*7, 53-56*).

Inserting protein into the interface

A higher MIP means that the hydrophobic domain of the protein can more easily insert and interact with the neutral core (triolein) of a phospholipid-coated oil droplet. The low MIP we observed for the mutant protein suggests that helix bundle unfolding plays a major role in protein interactions at the oil-phospholipid interface. Most of the hydrophobic residues are located in the interior of the helix bundle. Helix bundle unfolding allows the hydrophobic amino acids access to the hydrophobic surface of the oil droplet.

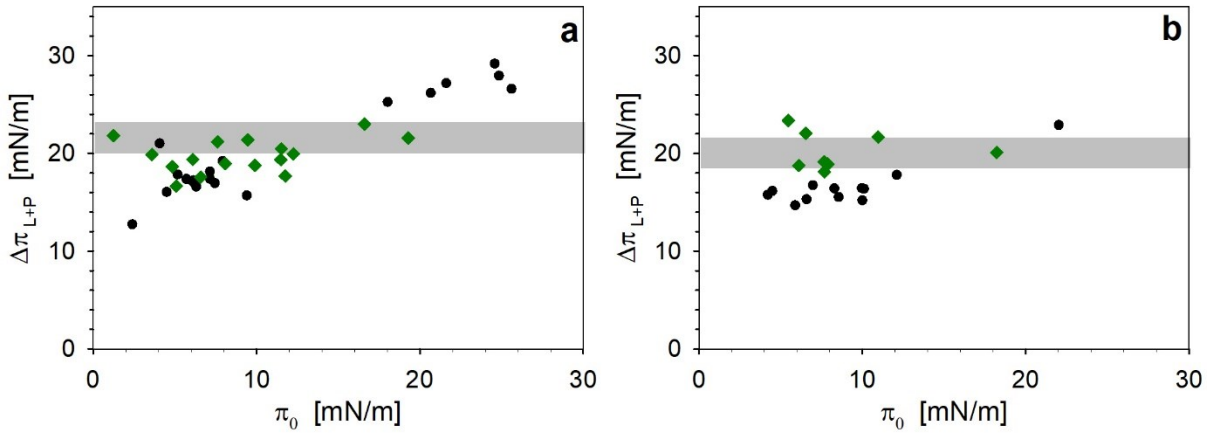

Figure 7. *The total change of surface tension due to both apoLp-III and lipid, as a function of the change of surface tension due to the lipid alone. The black circles indicate POPC alone; the green diamonds indicate a 9:1 POPC:POPA lipid composition. The grey rectangle indicates the change of surface tension due to the protein alone, along with its standard deviation. (a) The protein is apoLp-III. (b) The protein is apoE. All experiments were performed in a buffer, pH ~7.2.*

The values for MIP for apoE 3 (NT) are highest for PC/POG while PC/POPE mixtures have significantly higher MIP values than that for the PC/POPA or the pure PC. The combined change

in pressure for the lipid and protein together, Figure 7 and Figure S7 (in the Supporting Information), gives additional insight. The combined pressure for PC and PC/PA remains approximately that of the apoE 3 (NT) protein alone. This is consistent with the protein forming islands within the lipid sea, with no cooperative effects (see Figure 8 and ref. (*32*)). Whereas, for PC/POPE and PC/POG (see Figure S6b) the combined pressure exceeds that of the protein, which implies cooperativity. ApoE3(NT) appears to require lipids with negative spontaneous curvature (i.e. POG and POPE) in order to adsorb cooperatively. In contrast, apoLp-III shows high insertion, and high cooperativity, for monolayers of pure PC and PC/POG. Previously, at the air-water interface, we showed that apoLp-III indeed favors interaction with diacylglycerol monolayers such as 1-palmitoyl, 2-oleoyl glycerol (*57*). Here, at the oil-phospholipid-aqueous interface we replicate this result, and additionally reveal a high degree of cooperativity for a PC monolayer. It is important to note that the natural interaction partner for apoLp-III is likely diacylglycerol as in

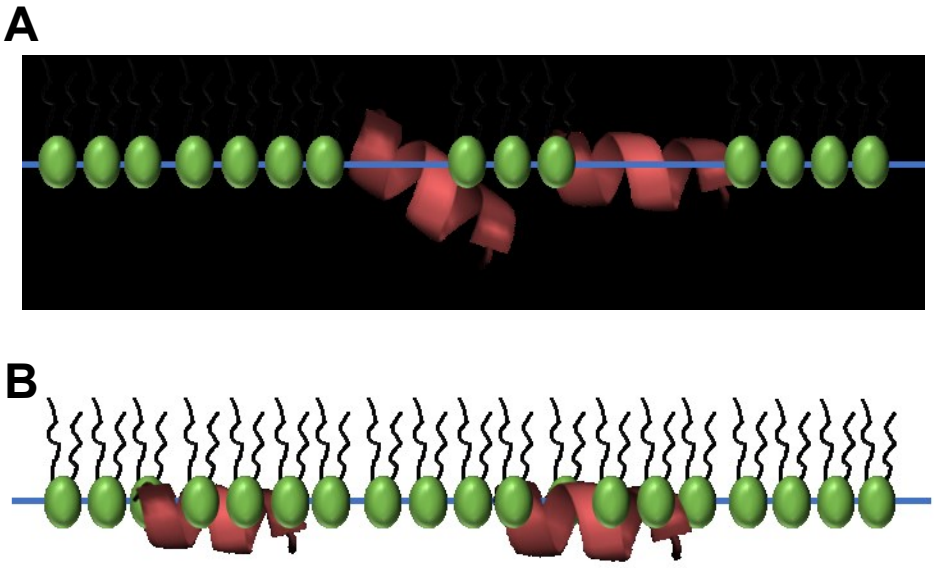

Figure 8. Illustration of non-cooperative interaction (A) and cooperative interaction (B) between the phospholipid monolayer and apolipoprotein at the oil-aqueous interface. Based on reference (32).

Locusta migratoria (the insect from which our apoLp-III was derived), lipophorin (insect lipoprotein) contains mainly diacylglycerol and not triacylglycerol.

The contrast between apoE 3 NT and apoLp-III indicates different modes of lipid insertion for the two distinct helix bundle protein domains. Large hydrophobic amino acid residues, such as tryptophan, phenylalanine, and tyrosine, facilitate protein interaction with the lipid interface (*58*). Indeed, apoE has a larger fraction of such residues compared to apoLp-III (Figures S4 and S5). This may explain, in part, the difference in adsorption behavior between apoE, and apoLp-III.

Stabilizing protein at the interface: dynamic surface tension measurements.

Oscillating the droplet volume, which also oscillates its surface area, models change in lipoprotein volume as lipids are taken up or consumed. In these experiments, the area change is limited by about a factor of 2.5 by the stability of the droplet on the syringe tip. How the surface pressure changes during this oscillation, the surface pressure isotherm, indicates the stability of the lipid/protein layers at the surface.

Lipid alone

All the lipid cases, in buffer or pure water, show similar behavior: the pressure increases continuously with decreasing area. On increasing the area again, the pressure abruptly drops. Such behavior is commonly seen in stiff lipid monolayers, which crack when decompressed. More or less hysteresis is observed; the most with the PC/PA mixture in pure water and the least with the PC/PE mixture in buffer. Subsequent compression/decompression cycles repeat the first one, which indicates that the monolayer has time to reorganize and that none of the material leaves the interface.

The surface pressure vs. droplet area isotherms for POPC/POG and POPC/POPA in pure water showed much more hysteresis than POPC and POPC/POPE or than any of these mixtures in buffer (See Figure 6 for PC:PA and Figure S4 for PC:POG). Larger hysteresis indicates more work to reorganize at the surface. Both POG and POPA pack more tightly in a membrane/monolayer (much smaller headgroup then PC and PE), and have a higher melting temperature. Hence the resulting monolayers containing POG and POPA are likely to be much stiffer, which follows the observed hysteresis. The hydrophobic interaction between the monolayer and triolein molecules also affects the work needed for these molecules to relax over time.

Lipid - Protein

The behavior of the lipid/protein monolayers is strikingly different. In the first compression, the surface pressure increases continuously only to a point, after which the slope of the increase decreases substantially. This behavior strongly suggests that the protein, perhaps with some lipid, collapses out of the interface above a certain pressure: At these pressures, the protein partially or completely leaves the interface, perhaps taking some of the phospholipid and/or triolein with it.

Upon decompression, the surface pressure of most of the protein/lipid films does not reverse this path but rather immediately decreases following a path nearly parallel to the initial compression curve. Further, the recompression isotherm often follows almost exactly the decompression curve. This behavior implies that the protein, perhaps with some lipid and/or triolein, irreversibly leaves the oil/water interface.

The isotherms in the presence of buffer, which decreases the Debye length (the characteristic length over which charge is screened by the redistribution of ions in solution), are significantly more reversible than those in water. (Note that the pH in this case is also higher.) The removal of

protein/lipid at a single high pressure is not as apparent in the presence of buffer in the lipid mixtures, compared to just POPC alone, and the isotherms are nearly reversible for modest compression, although they become irreversible at higher compressions.

The PC:PA system behaved distinctly differently. With the protein on the interface, in water, the first compression leads to irreversible rearrangement of the lipid layer: the minimum pressure decreases from 25 to 5 mN/m. However, succeeding compression/decompression cycles are reversible, so that after the first compression the lipids and proteins are almost certainly staying partially bound to the interface. The presence of PA thus seems to facilitate rebinding of the protein to the interface. We speculate that the negative charge on PA facilitates rebinding. This is consistent with the observed value of $\Delta\pi_{max}$, which is highest for the POPA containing monolayer.

Conclusion

These results lead to one clear conclusion and suggests several others. Comparison of the locked and unlocked versions of apoLp-III clearly indicates the importance of helix-bundle unfolding to insertion of the protein into the oil/phospholipid/aqueous interface. Unfolding the helix exposes the hydrophobic residues at the interior, while allowing the charged residues to remain in contact with the aqueous phase.

Negative charge attracts both proteins to the phospholipid-coated triolein interface. It also brought protein (apoLp-III) back to the interface in dynamic compression-decompression experiments. However, negative charge also discouraged cooperative interaction in highly packed lipid-protein monolayers. In these PA containing monolayers, the protein appears to form islands within the lipid monolayer, perhaps due to electrostatic repulsion.

On the other hand, negative spontaneous curvature of POPE and POG, which tends to induce defects in the phospholipid monolayer, encourages cooperative interaction for apoE, and partially for apoLp-III. ApoLp-III appears to have a special interaction with diacylglycerol, the natural interaction partner for this protein. Stiffness of the lipid monolayer plays an important role in reorganization of the lipid-protein monolayer upon compression and expansion of the lipid droplet.

MD simulations would be useful to confirm and supplement our experimental findings. MD simulations have already revealed important insights into the structure of the phospholipid monolayer at a triolein interface. For example, interdigitation of triolein with the acyl chains of the phospholipid monolayer induces defects in the monolayer not present in lipid bilayers (*59*). Additionally, large hydrophobic amino acid residues were shown to have a preferential interaction with defects in the phospholipid monolayer (*6*). Future MD simulations using apoLp-III and apoE will provide further insight into the general mechanisms by which neutral lipid binding proteins recognize and bind to the phospholipid-oil interface.

Acknowledgments

We gratefully acknowledge Drs. Paul Weers and Vasanthi Narayanaswami for providing us with apoLp-III and the N terminus of apoE. We would also like to thank Amber Titus for critical discussion and assistance with droplet tensiometry. This work was supported by the National Science Foundation under Grant No. CHE-1808281. This work was completed while EKM served at the National Science Foundation.

Supporting Information

Liquid droplet tensiometer set-up; static and dynamic insertion isotherms, and protein α-helix wheel diagrams and calculated hydrophobic moments.

References:

1. Hauser, P. S.; Narayanaswami, V.; Ryan, R. O. Apolipoprotein E: from lipid transport to neurobiology. *Prog. Lipid Res.* **2011,** *50*, 62-74.
2. Narayanaswami, V.; Maiorano, J. N.; Dhanasekaran, P.; Ryan, R. O.; Phillips, M. C.; Lund-Katz, S.; Davidson, W. S. Helix orientation of the functional domains in apolipoprotein E in discoidal high density lipoprotein particles. *J. Biol. Chem.* **2004,** *279*, 14273-14279.
3. Smith, L. E.; Segrest, J. P.; Davidson, W. S. Helical domains that mediate lipid solubilization and ABCA1-specific cholesterol efflux in apolipoproteins C-I and A-II. *J. Lipid Res.* **2013,** *54*, 1939-1948.
4. Segrest, J. P.; Jackson, R. L.; Morrisett, J. D.; Gotto, A. M., Jr. A molecular theory of lipid-protein interactions in the plasma lipoproteins. *FEBS Lett.* **1974,** *38*, 247-258.
5. Narayanaswami, V.; Wang, J.; Schieve, D.; Kay, C. M.; Ryan, R. O. A molecular trigger of lipid binding-induced opening of a helix bundle exchangeable apolipoprotein. *Proc. Natl. Acad. Sci. U. S. A.* **1999,** *96*, 4366-4371.
6. Prevost, C.; Sharp, M. E.; Kory, N.; Lin, Q.; Voth, G. A.; Farese, R. V. Jr.; Walther, T. C. Mechanism and Determinants of Amphipathic Helix-Containing Protein Targeting to Lipid Droplets. *Dev. Cell* **2018,** *44*, 73-86 e74.
7. Narayanaswami, V.; Wang, J.; Kay, C. M.; Scraba, D. G.; Ryan, R. O. Disulfide bond engineering to monitor conformational opening of apolipophorin III during lipid binding. *J. Biol. Chem.* **1996,** *271*, 26855-26862.
8. Eichner, J. E.; Dunn, S. T.; Perveen, G.; Thompson, D. M.; Stewart, K. E.; Stroehla, B. C. Apolipoprotein E polymorphism and cardiovascular disease: a HuGE review. *Am. J. Epidemiol.* **2002,** *155*, 487-495.
9. Mahley, R. W.; Huang, Y.; Rall, S. C., Jr. Pathogenesis of type III hyperlipoproteinemia (dysbetalipoproteinemia). Questions, quandaries, and paradoxes. *J. Lipid Res.* **1999,** *40*, 1933-1949.
10. Zhao, W.; Dumanis, S. B.; Tamboli, I. Y.; Rodriguez, G. A.; Jo Ladu, M.; Moussa, C. E.; William Rebeck, G. Human APOE genotype affects intraneuronal Abeta1-42 accumulation in a lentiviral gene transfer model. *Hum. Mol. Genet.* **2014,** *23*, 1365-1375.
11. Phillips, M. C. Apolipoprotein E isoforms and lipoprotein metabolism. *IUBMB Life* **2014,** *66*, 616-623.
12. Utermann, G. Apolipoprotein E polymorphism in health and disease. *Am. Heart J.* **1987,** *113*, 433-440.
13. Holtzman, D. M.; Herz, J.; Bu, G. Apolipoprotein E and apolipoprotein E receptors: normal biology and roles in Alzheimer disease. *Cold Spring Harb. Perspect. Med.* **2012,** *2*, a006312.
14. Liu, C. C.; Kanekiyo, T.; Xu, H., Bu, G. Apolipoprotein E and Alzheimer disease: risk, mechanisms and therapy. *Nat. Rev. Neurol.* **2013,** *9*, 106-118.
15. Breiter, D. R.; Kanost, M. R.; Benning, M. M.; Wesenberg, G.; Law, J. H.; Wells, M. A.; Rayment, I.; Holden, H. M. Molecular structure of an apolipoprotein determined at 2.5-A resolution. *Biochemistry* **1991,** *30*, 603-608.
16. Zdybicka-Barabas, A.; Cytrynska, M. Apolipophorins and insects immune response. *Isj-Invert. Surviv. J.* **2013,** *10*, 58-68.
17. Wan, C. P.; Chiu, M. H.; Wu, X.; Lee, S. K.; Prenner, E. J.: Weers, P. M. Apolipoprotein-induced conversion of phosphatidylcholine bilayer vesicles into nanodisks. *Biochim. Biophys. Acta* **2011,** *1808*, 606-613.

18. Weers, P. M.; Prenner, E. J.; Curic, S.; Lohmeier-Vogel, E. M. A laboratory exercise to illustrate protein-membrane interactions. *Biochem. Mol. Biol. Educ.* **2016,** *44*, 86-94.
19. Raussens, V.; Narayanaswami, V.; Goormaghtigh, E.; Ryan, R. O.; Ruysschaert, J. M. Alignment of the apolipophorin-III alpha-helices in complex with dimyristoylphosphatidylcholine. A unique spatial orientation. *J. Biol. Chem.* **1995,** *270*, 12542-12547.
20. Wientzek, M.; Kay, C. M.; Oikawa, K.; Ryan, R. O. Binding of insect apolipophorin III to dimyristoylphosphatidylcholine vesicles. Evidence for a conformational change. *J. Biol. Chem.* **1994,** *269*, 4605-4612.
21. Small, D. M.; Wang, L.; Mitsche, M. A. The adsorption of biological peptides and proteins at the oil/water interface. A potentially important but largely unexplored field. *J. Lipid Res.* **2009,** *50 Suppl*, S329-334.
22. Small, D. M. A 27AA peptide designed from the consensus sequence of 41 B-strands in the first B-sheet region of apolipoprotein B (AA 968-1881) binds strongly, to a hydrocarbon/water interface. *Biophys. J.* **2001,** *80*, 186a-186a.
23. Wang, L.; Small, D. M. Interfacial properties of amphipathic beta strand consensus peptides of apolipoprotein B at oil/water interfaces. *J. Lipid Res.* **2004,** *45*, 1704-1715.
24. Wang, L.; Walsh, M. T.; Small, D. M. Apolipoprotein B is conformationally flexible but anchored at a triolein/water interface: a possible model for lipoprotein surfaces. *Proc. Natl. Acad. Sci. U. S. A.* **2006,** *103*, 6871-6876.
25. Meyers, N. L.; Larsson, M.; Olivecrona, G.; Small, D. M. A Pressure-dependent Model for the Regulation of Lipoprotein Lipase by Apolipoprotein C-II. *J. Biol. Chem.* **2015,** *290*, 18029-18044.
26. Meyers, N. L.; Wang, L.; Small, D. M. Apolipoprotein C-I binds more strongly to phospholipid/triolein/water than triolein/water interfaces: a possible model for inhibiting cholesterol ester transfer protein activity and triacylglycerol-rich lipoprotein uptake. *Biochemistry* **2012,** *51*, 1238-1248.
27. Beck, W. H.; Adams, C. P.; Biglang-Awa, I. M.; Patel, A. B.; Vincent, H.; Haas-Stapleton, E. J.; Weers, P. M. Apolipoprotein A-I binding to anionic vesicles and lipopolysaccharides: role for lysine residues in antimicrobial properties. *Biochim. Biophys. Acta* **2013,** *1828*, 1503-1510.
28. Horn, J.; Ellena, R.; Tran, J.; Narayanaswami, V.; Weers, P. Characterization of the C-Terminal Domain of human apolipoprotein A-I via a novel apolipoprotein chimera. *Faseb J.* **2015,** *29*, 886.10.
29. Sallee, D.; Horn, J.; Weers, P. A novel method for expression and purification of the C-terminal domain of apolipoprotein A-I. *Faseb J.* **2015,** *29,* LB98.
30. Wang, L. B.; Mei, X. H.; Atkinson, D.; Small, D. M. Surface behavior of apolipoprotein A-I and its deletion mutants at model lipoprotein interfaces. *J. Lipid Res.* **2014,** *55*, 478-492.
31. Richardson, P. E.; Manchekar, M.; Dashti, N.; Jones, M. K.; Beigneux, A.; Young, S. G.; Harvey, S. C.; Segrest, J. P. Assembly of lipoprotein particles containing apolipoprotein-B: structural model for the nascent lipoprotein particle. *Biophys. J.* **2005,** *88*, 2789-2800.
32. Mirheydari, M.; Mann, E. K.; Kooijman, E. E. Interaction of a model apolipoprotein, apoLp-III, with an oil-phospholipid interface. *Biochim. Biophys. Acta* **2018,** *1860*, 396-406.
33. Leikin, S.; Kozlov, M. M.; Fuller, N. L.; Rand, R. P. Measured effects of diacylglycerol on structural and elastic properties of phospholipid membranes. **1996,** *Biophys. J. 71*, 2623-2632.
34. Kooijman, E. E.; Chupin, V.; Fuller, N. L.; Kozlov, M. M.; de Kruijff, B.; Burger, K. N. J.; Rand, P. R. Spontaneous curvature of phosphatidic acid and lysophosphatidic acid. *Biochemistry* **2005,** *44*, 2097-2102.
35. Kollmitzer, B.; Heftberger, P.; Rappolt, M.; Pabst, G. Monolayer spontaneous curvature of raft-forming membrane lipids. *Soft Matter* **2013,** *9*, 10877-10884.

36. Kalantarian, A.; Ninomiya, H.; Saad, S. M.; David, R.; Winklbauer, R.; Neumann, A. W. Axisymmetric drop shape analysis for estimating the surface tension of cell aggregates by centrifugation. *Biophys. J.* **2009,** *96*, 1606-1616.
37. Yang, J.; Yu, K.; Zuo, Y. Y. Accuracy of Axisymmetric Drop Shape Analysis in Determining Surface and Interfacial Tensions. *Langmuir* **2017,** *33*, 8914-8923.
38. Titus, A. R.; Ridgway, E. N.; Douglas, R.; Sánchez-Brenes, E.; Mann, E. K.; Kooijman, E. E. The C-terminus of perilipin 3 shows distinct lipid binding at oil/phospholipid-aqueous interfaces. *Membranes* **2021,** *11*, 265.
39. Bartz, R.; Li, W. H.; Venables, B.; Zehmer, J. K.; Roth, M. R.; Welti, R.; Anderson, R. G.; Liu, P.; Chapman, K. D. Lipidomics reveals that adiposomes store ether lipids and mediate phospholipid traffic. *J. Lipid Res.* **2007,** *48*, 837-847.
40. Luckey, M. *Membrane structural biology : with biochemical and biophysical foundations*, Second edition. ed.
41. Meyers, N. L.; Larsson, M.; Vorrsjo, E.; Olivecrona, G.; Small, D. M. Aromatic residues in the C terminus of apolipoprotein C-III mediate lipid binding and LPL inhibition. *J. Lipid Res.* **2017,** *58*, 840-852.
42. Calvez, P.; Bussieres, S.; Eric, D.; Salesse, C. Parameters modulating the maximum insertion pressure of proteins and peptides in lipid monolayers. *Biochimie* **2009,** *91*, 718-733.
43. Ledford, A. S.; Cook, V. A.; Shelness, G. S.; Weinberg, R. B. Structural and dynamic interfacial properties of the lipoprotein initiating domain of apolipoprotein B. *J. Lipid Res.* **2009,** *50*, 108-115.
44. Oliveira, R. G.; Calderon, R. O.; Maggio, B. Surface behavior of myelin monolayers. *Biochim. Biophys. Acta* **1998,** *1370*, 127-137.
45. Kooijman, E. E.; Carter, K. M.; van Laar, E. G.; Chupin, V.; Burger, K. N.; de Kruijff, B. What makes the bioactive lipids phosphatidic acid and lysophosphatidic acid so special? *Biochemistry* **2005,** *44*, 17007-17015.
46. Kooijman, E. E.; Chupin, V.; de Kruijff, B.; Burger, K. N. Modulation of membrane curvature by phosphatidic acid and lysophosphatidic acid. *Traffic* **2003,** *4*, 162-174.
47. de Kruijff, B. Lipid polymorphism and biomembrane function. *Curr. Opin. Chem. Biol.* **1997,** *1*, 564-569.
48. Putta, P.; Rankenberg, J.; Korver, R. A.; van Wijk, R.; Munnik, T.; Testerink, C.; Kooijman, E. E. Phosphatidic acid binding proteins display differential binding as a function of membrane curvature stress and chemical properties. *Biochim. Biophys. Acta* **2016,** *1858*, 2709-2716.
49. van den Brink-van der Laan, E.; Killian, J. A.; de Kruijff, B. Nonbilayer lipids affect peripheral and integral membrane proteins via changes in the lateral pressure profile. *Biochim. Biophys. Acta* **2004,** *1666*, 275-288.
50. daCosta, C. J.; Ogrel, A. A.; McCardy, E. A.; Blanton, M. P.; Baenziger, J. E. Lipid-protein interactions at the nicotinic acetylcholine receptor. A functional coupling between nicotinic receptors and phosphatidic acid-containing lipid bilayers. *J. Biol. Chem.* **2002,** *277*, 201-208.
51. Ghimire, C.; Koirala, D.; Mathis, M. B.; Kooijman, E. E.; Mao, H. Controlled particle collision leads to direct observation of docking and fusion of lipid droplets in an optical trap. *Langmuir* **2014,** *30*, 1370-1375.
52. Marinova, K. G.; Alargova, R. G.; Denkov, N. D.; Velev, O. D.; Petsev, D. N.; Ivanov, I. B.; Borwankar, R. P. Charging of oil-water interfaces due to spontaneous adsorption of hydroxyl ions. *Langmuir* **1996,** *12*, 2045-2051.
53. Narayanaswami, V.; Frolov, A.; Schroeder, F.; Oikawa, K.; Kay, C. M.; Ryan, R. O. Fluorescence studies of lipid association-induced conformational adaptations of an exchangeable amphipathic apolipoprotein. *Arch. Biochem. Biophys.* **1996,** *334*, 143-150.

54. Weers, P. M.; Kay, C. M.; Ryan, R. O. Conformational changes of an exchangeable apolipoprotein, apolipophorin III from Locusta migratoria, at low pH: correlation with lipid binding. *Biochemistry* **2001,** *40*, 7754-7760.
55. Weers, P. M.; Narayanaswami, V.; Kay, C. M.; Ryan, R. O. Interaction of an exchangeable apolipoprotein with phospholipid vesicles and lipoprotein particles. Role of leucines 32, 34, and 95 in Locusta migratoria apolipophorin III. *J. Biol. Chem.* **1999,** *274*, 21804-21810.
56. Weers, P. M.; Ryan, R. O. Apolipophorin III: a lipid-triggered molecular switch. *Insect Biochem. Mol. Biol.* **2003,** *33*, 1249-1260.
57. Rathnayake, S. S.; Mirheydari, M.; Schulte, A.; Gillahan, J. E.; Gentit, T.; Phillips, A. N.; Okonkwo, R. K.; Burger, K. N.; Mann, E. K.; Vaknin, D.; et al. Insertion of apoLp-III into a lipid monolayer is more favorable for saturated, more ordered, acyl-chains. *Biochim. Biophys. Acta.* **2014,** *1838*, 482-492.
58. Copic, A.; Antoine-Bally, S.; Gimenez-Andres, M.; La Torre Garay, C.; Antonny, B.; Manni, M. M.; Pagnotta, S.; Guihot, J.; Jackson, C. L. A giant amphipathic helix from a perilipin that is adapted for coating lipid droplets. *Nat. Commun.* **2018,** *9*, 1332.
59. Bacle, A.; Gautier, R.; Jackson, C. L.; Fuchs, P. F. J.; Vanni, S. Interdigitation between triglycerides and lipids modulates surface properties of lipid droplets. *Biophys. J.* **2017,** *112*, 1417-1430.

Supporting Information

Interaction of Two Amphipathic α-Helix Bundle Proteins, ApoLp-III and ApoE 3, With the Oil-Aqueous Interface

Mona Mirheydari[1], Priya Putta[2], Elizabeth K. Mann[1], Edgar E. Kooijman[2*]

Kent State University, [1]Physics Department, and [2]Department of Biological Sciences, PO Box 5190, Kent, OH 44242

[*]corresponding author, ekooijma@kent.edu

Experimental Set-Up

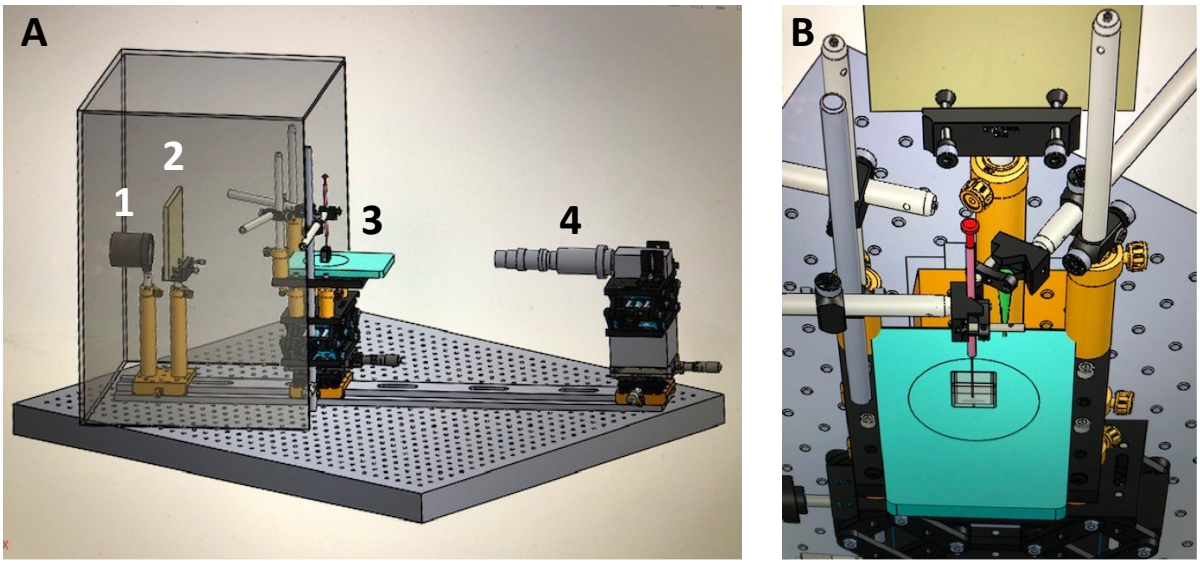

Figure S1*. Schematic of our home-built droplet tensiometer. A) Overview. Indicated are 1. Back lid light source, 2. Diffuser, 3. Cuvette and syringe platform, 4. Camera. B) Detailed overview of the cuvette and syringe set-up. Schema curtesy of Bentley Wall.*

Protein alone at oil/water interface

The surface tension of a triolein droplet was measured in the presence of 0.1 nmole/mL of protein in solution with either pure water or with Tris buffer: 10mM Tris-HCl, 150 mM KCl, 0.2 mM EDTA at pH7.2. Measurements were taken after ~1 hour.

	Δπ [mN/m]	
	apoE 3 (NT)	**apoLp-III**
water		**21.7± 1.5**
buffer	**20.2± 1.2**	**21.2± 1.2**

Table S1: The change in surface tension in the presence of 0.1 nmole/mL of one of the protein, apoE 3 (NT) or apoLp-III.

Insertion of protein into different lipid monolayers on triolein droplets.

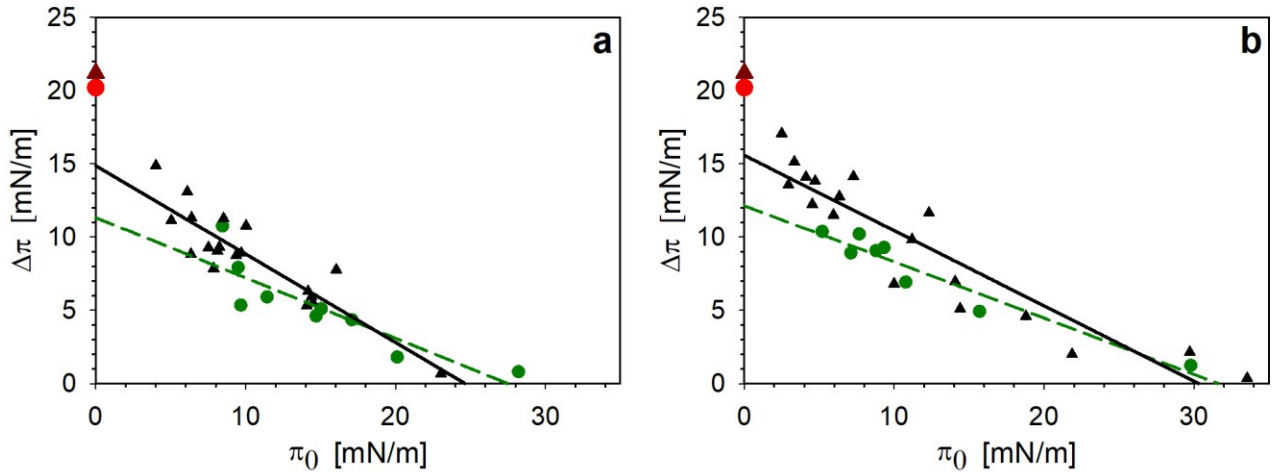

Figure S2*. Comparison of the insertion of apoE 3(NT) (green circles) and apoLp-III (black triangles) into a) PC:PE monolayers and b) PC:POG monolayers. Red symbols at* $\pi_0 = 0$ *correspond to protein alone, without phospholipids (see Table S1). Tris buffer: 10mM Tris-HCl, 150 mM KCl, 0.2 mM EDTA at pH7.2.*

The dynamics of a protein-phospholipid film on a triolein droplet:

The data in Figures S3 and S4 were taken in the same way as the data in Figures 5 and 6, but with different lipid mixtures as indicated.

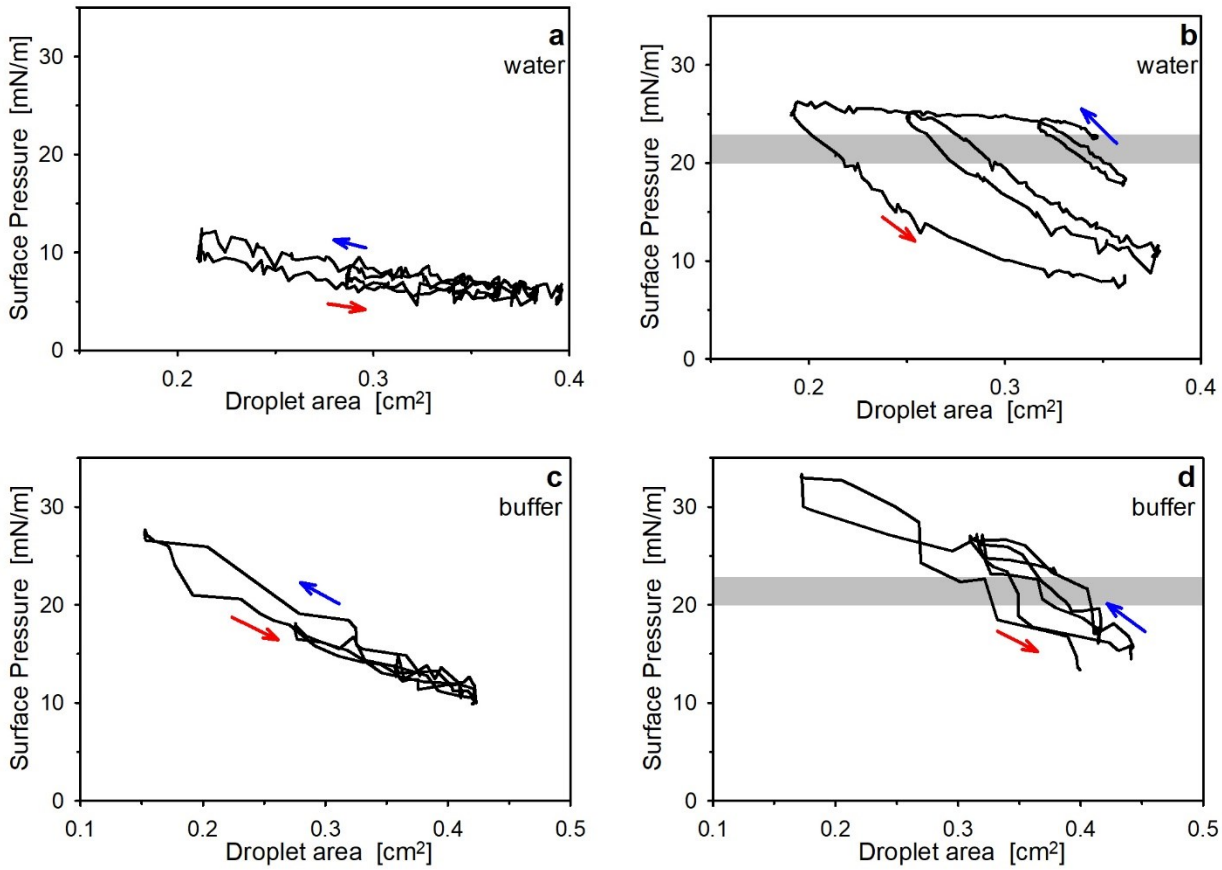

Figure S3. *Comparison of successive compression and decompression isotherms for an oil droplet first after coating with a 9:1 POPC/POPE lipid (a,c) mixture, and then after apoLp III protein insertion (b,d). The same experiments are performed with the droplet in pure water (a,b) and in a physiologically relevant buffer, pH ~7.2 (c,d).Grey bars in (b,d) represents surface pressure by just the protein interacting with the neat oil interface.*

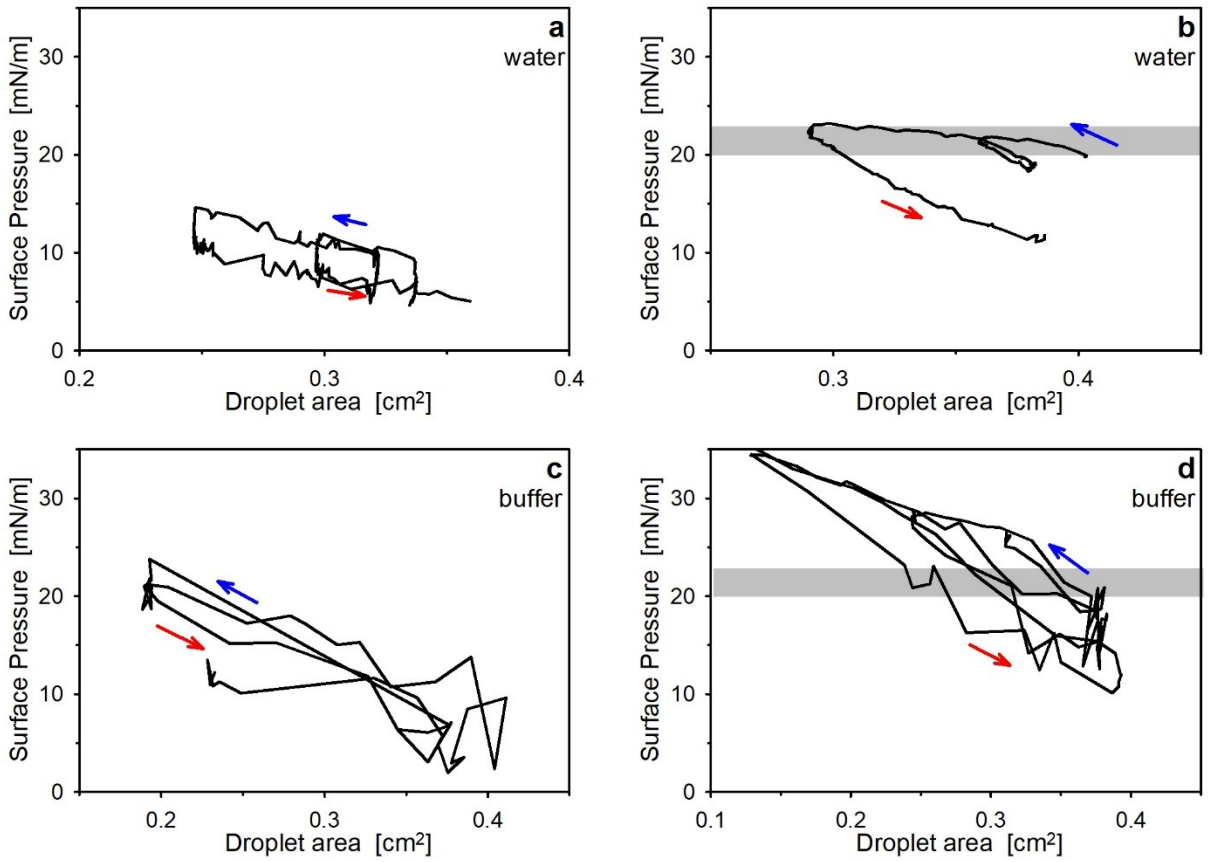

Figure S4. *Comparison of successive compression and decompression isotherms for an oil droplet first after coating with a 9:1 POPC/POG lipid (a,c) mixture, and then after apoLp III protein insertion (b,d). The same experiments are performed with the droplet in pure water (a,b) and in a physiologically relevant buffer, pH ~7.2 (c,d). Grey bars in (b,d) represents surface pressure by just the protein interacting with the neat oil interface.*

Helical wheel representations of the two proteins.

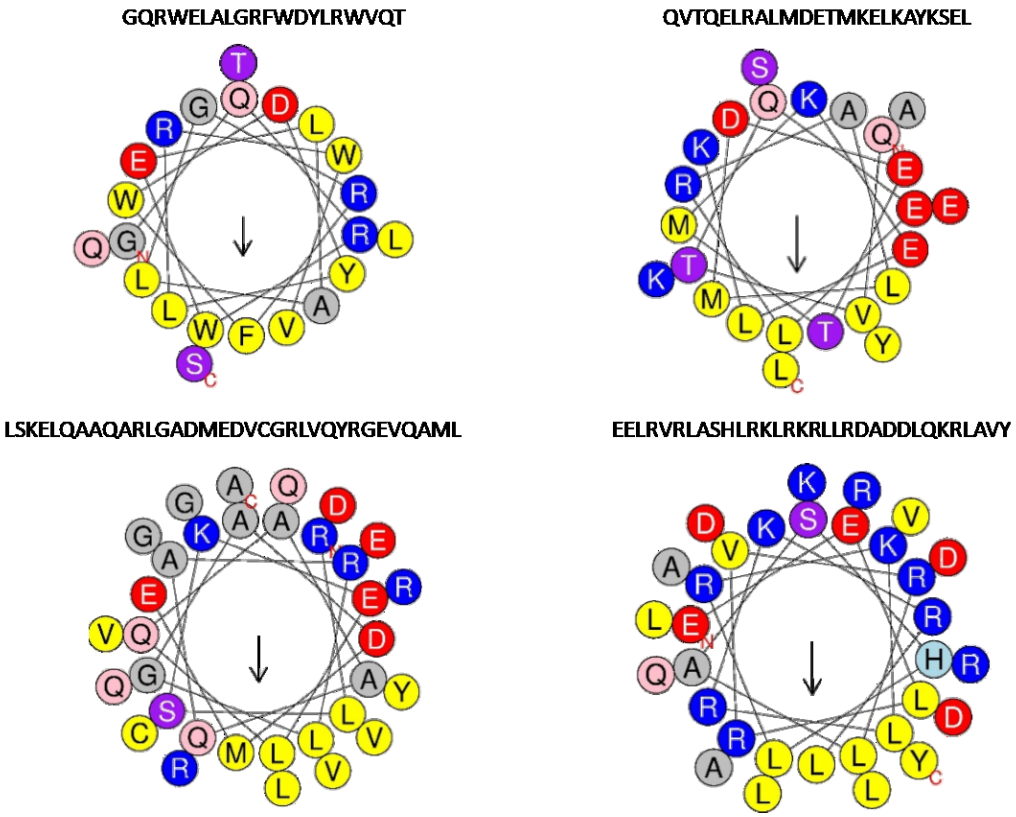

	Net Charge	Hydrophobicity	Hydrophobic moment
1 st Helix	+1	0.576	0.355
2nd Helix	-1	0.200	0.466
3rd Helix	0	0.126	0.402
4th Helix	+6	0.130	0.426

Figure S5*. Helical wheel structure for apoE 3(NT). Each helix is drawn separately. Hydrophobic surfaces are marked with yellow and gray circles, while, polar amino acids are displayed with red and blue colors. Table shows the value for hydrophobicity, hydrophobic moment and net charge for each helix. The figure was prepared using HeliQuest program from protein data bank 1nfn.pdb.*

1st Helix:
IAEAVQQLNHTIVNAAHELHETLG

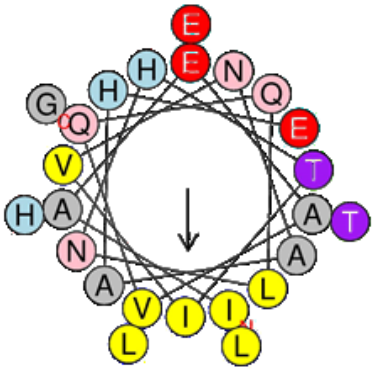

2nd Helix:
LNLLTEQANAFKTKIAEVTTSLKQE

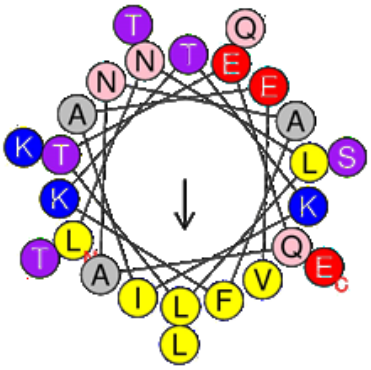

3rd Helix:

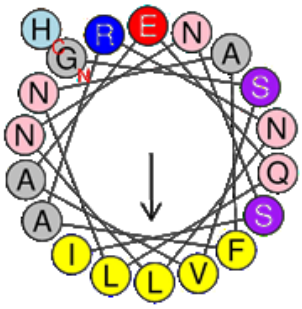

4th Helix:
GSVAEQLNAFARNLNNSIH

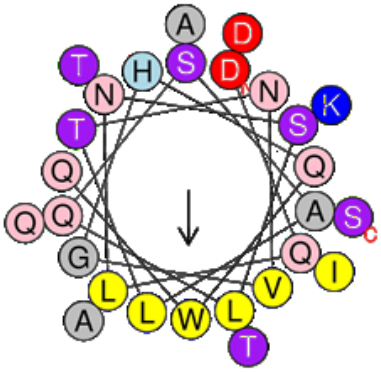

5th Helix:
WAPVQSALQEAAEKTKEAAANLQNSIQSAVQ

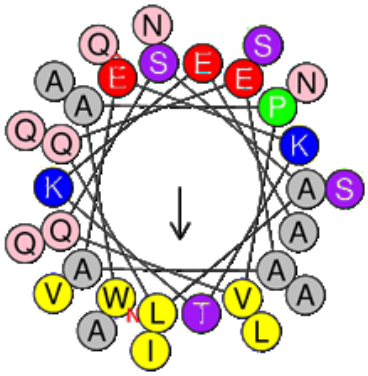

	Net Charge	Hydrophobicity $\langle H \rangle$	Hydrophobic moment $\langle \mu H \rangle$
1st helix	0	0.405	0.474
2nd helix	0	0.280	0.380
3rd helix	+1	0.259	0.510
4th helix	0	0.269	0.413
5th helix	-1	0.227	0.400

Figure S6: *Helical wheel structure for apoLpIII. Each helix is drawn separately. Hydrophobic surfaces are marked with yellow and gray circles while polar amino acids are displayed with red and blue colors. Table shows the value for hydrophobicity, hydrophobic moment and net charge for each helix. The figure was prepared form protein data bank 1ls4.pdb.*

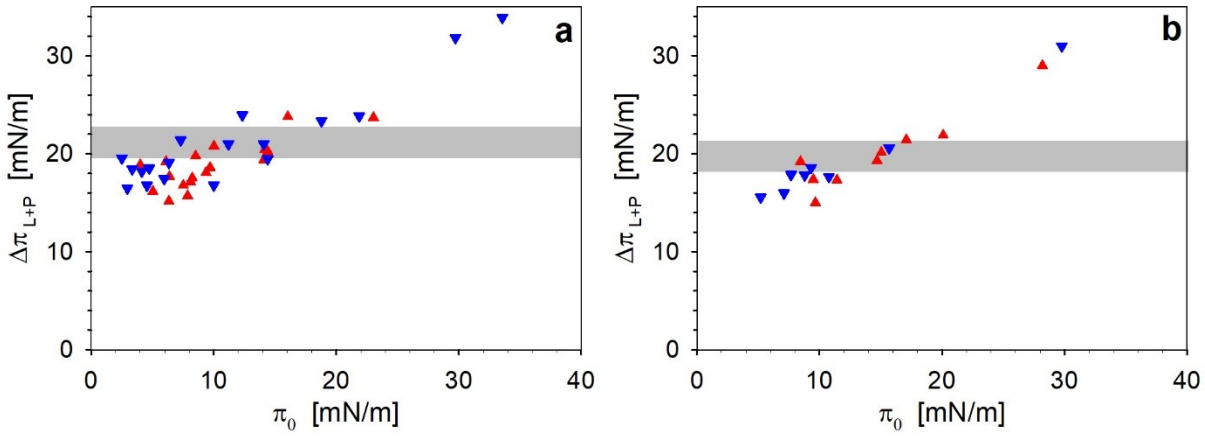

Figure S7. *The total change of surface tension due to both protein and lipid, as a function of the change of surface tension due to the lipid alone. The red point-up triangles indicate a 9:1 POPC:POPE lipid composition; the blue point-down triangles indicate a 9:1 POPC:POG lipid composition. The grey bar indicates the change of surface tension due to the protein alone, along with its standard deviation. (a) The protein is apoLpIII. (b) The protein is apoE. All experiments were performed in a buffer, pH ~7.2.*